Mingsakul, Thaworn; Surachon, Preeyaporn; Somana, Reon
Conduction System in the Swine Heart: Essential Landmarks for Gross Dissection
Acta Scientiae Veterinariae, vol. 42, núm. 1, enero, 2014, pp. 1-8
Universidade Federal do Rio Grande do Sul
Porto Alegre, Brasil

Acta Scientiae Veterinariae,
ISSN (Printed Version): 1678-0345
ActaSciVet@ufrgs.br
Universidade Federal do Rio Grande do Sul
Brasil

Acta Scientiae Veterinariae, 2014. 42: 1211.

RESEARCH ARTICLE
Pub. 1211

ISSN 1679-9216

Conduction System in the Swine Heart: Essential Landmarks for Gross Dissection

Thaworn Mingsakul[1], Preeyaporn Surachon[1] & Reon Somana[2]

ABSTRACT

***Background*:** The components of the cardiac conduction system (CCS) were discovered almost two centuries and presented in the diagrammatic forms. This should be due to the difficulty in distinguishing the CCS from the surrounding cardiac tissues and the lack of information concerning the precise landmarks for gross dissection. Furthermore the CCS in pig, the animal regarded as a suitable model for the assessment of catheter based intervention, has not been reported. The aims of the present study were to demonstrate the gross anatomic architecture of CCS in the swine heart, and to provide the valuable landmarks for the gross anatomic dissection of the CCS.

***Materials, Methods & Results*:** Twenty hearts of adult Large White pigs (*Sus Scrofa domesticus*) were used. Fifteen hearts were elucidated by gross anatomic dissection. The tissue blocks of the sinoatrial node (SAN) and atrioventricular conduction tissue of the five hearts were prepared for histological investigation by staining with Masson's trichrome. It was found histologically that the cardiac conduction tissues were clearly distinguishable from the surrounding cardiac myocardium and connective tissue. Moreover, the histological information also navigated the location and anatomical architecture of the CCS which provided essential guideline for gross dissection. The SAN was somewhat spindle in shape which embedded in epicardial connective tissue of the terminal sulcus. In some cases, it was quite difficult to identifythe SAN, so the sinoatrial node artery was used as a clue. The AVN was an elliptical shaped which situated in subendocardial tissue at apex of the triangle of Koch on the atrial surface of the central fibrous body. The distal extremity of the AVN extended into the central fibrous body to form the penetrating bundle of His. At the boundary between the membranous and muscular parts of the interventricular septum, the AV bundle of His divided into the right (RBB) and left bundle branches (LBB). The RBB coursed downward in the muscular part of the interventricular septum around the base of the anterior papillary muscle and then traveled along the septomarginal trabecula. The LBB passed through the lower rim of the membranous septum and appeared on the endocardial surface of the left ventricle at the commissure between the right coronary and non-coronary leaflets of the aortic valve. However, intramural branches of the Purkinje network could not be identified.

***Discussion*:** The present study reveals that the anatomic architecture and location of the CCS in the pig heart could be demonstrated by gross anatomic dissection, and the essential landmarks for gross investigation were suggested. The crucial landmarks for the identification of the SAN, the AV conduction tissue and the LBB are the superior cavoatrial junction, the attachment of the septal leaflet adjoining the membranous septum, and the junction between the right coronary and noncoronary leaflets of the aortic valve, respectively. These landmarks are useful not only for gross anatomic dissection of the CCS in the pig heart but also provide the fundamental information for cardiac arrhythmia and sudden death experimentation in this animal. Therefore these findings should be valuable for anatomists, cardiovascular researchers and veterinary clinicians as well as veterinary and medical students.

Keywords: cardiac conduction system, sinoatrial node, atrioventricular node, atrioventricular bundle, swine heart.

Received: 4 April 2014 Accepted: 18 September 2014 Published: 28 September 2014

[1]Department of Anatomy, Faculty of Veterinary Medicine, Khon Kaen University, Khon Kaen province, Thailand. [2]Faculty of Medicine, Mahasarakham University, Mahasarakham province, 40115, Thailand. CORRESPONDENCE: T. Mingsakul [thamin@kku.ac.th - Fax: +66 (0)4-336-4496]. Department of Anatomy, Faculty of Veterinary Medicine, Khon Kaen University, Khon Kaen province, 40002, Thailand.

INTRODUCTION

Anatomical structure of the cardiac conduction system (CCS) has been introduced since nineteenth century. The Purkinje network was discovered by Purkinje in 1839 and in 1893 the atiroventricular bundle was demonstrated by His [22]. In 1906, Tawara [2] identified the atrioventricular node, and right and left bundle branches. Thereafter, Keith and Flack [15] introduced the sinoatrial node. The CCS components were discovered almost two centuries; however, most of their locations and morphologies have been displayed as the diagrammatic illustrations based on histological sections [3,9] or serial reconstructions [1,9,22]. It is very difficult to distinguish the conduction tissues from the surrounding cardiac tissues by gross dissection due to the lack of information to used as critical landmarks. Although a number of gross anatomical investigations of the human CCS have been demonstrated [13,24], those in animals do not presented, especially during the gross anatomy dissection classes of small and large animals.

It is interesting to elucidate the gross anatomical structures of the CCS in the pig heart which regarded as a suitable animal model for the assessment of catheter-based intervention [23] and myocardial infarction [7]. The aims of the present study are to demonstrate the gross anatomic architectures of CCS in the swine heart, and to provide the valuable landmarks to approach the CCS in gross dissection and clinical investigation.

MATERIALS AND METHODS

Twenty normal hearts of adult Large White pigs (*Sus Scrofa domesticus*), weighing between 90-120 kg, were used. They were obtained from the slaughter house in Khon Kaen province, Thailand. The cardiac chambers were opened before rinsing in tap water to completely wash the blood out. The right atrium and ventricle were exposed by making an incision beginning from the tip of the right atrial appendage to the inferior border of the right atrium. Then the incision was extended through the acute margin of the right ventricle to the apex of the heart. The left ventricle was opened by making a longitudinal incision from the ascending aorta and cut downward through the wall of the left ventricle along a line slightly to the left of the anterior interventricular sulcus to the apex of the heart.

The specimens were divided into Group I (five hearts) for light microscopic study, and Group II (fifteen hearts) for gross anatomic dissection. In Group I, the tissue blocks of the SAN and AV conduction tissue were fixed in 10% neutral-buffered formalin for 4 days, and then were prepared according to histological standard procedures. The sinoatrial node tissue block was sectioned perpendicular to the long axis of the terminal crest (Figure 3A) whereas the atrioventricular conduction tissue block was cut perpendicular to the attachment of the septal leaflet (Figure 5A). After staining with Masson's Trichrome, the tissue sections were examined and photographed under light microscope (PrimoStar, Carl Zeiss[1]) with AxioCam ERc5S imaging system (Axio Vision LE)[2]. In Group II, the hearts were immerged in 10% neutral formalin for 7 days before the AV conduction tissue was investigated by gross anatomic dissection and then photographed.

RESULTS

Prior histological and gross anatomic investigations of the CCS performed, the related and helpful anatomic structures to localize the conduction tissue were identified. In figure 1 the terminal crest was situated between the sinus venarum and right atrial appendage. It was a vertical crest posing on endocardial aspect of the right atrium, which corresponding to the terminal sulcus on epicardial aspect where the SAN situated. A triangle of Koch was also identified, because of the AVN situating at its apex. The apex of this triangle was bordered anteriorly by the attachment of the septal leaflet of the tricuspid valve and posteriorly by a fibrous tendon of Todaro. Base of the triangle was confined by the coronary sinus orifice. Moreover, the membranous and muscular portions of the interventricular septm as well as septomarginalis trabecula were clarified (Figure 1).

The tissue sections stained with Masson's trichrome distinctly differentiated that the cardiac myocytes, connective tissue and cardiac conduction tissue were red, blue and pink, respectively. It was presented that the cardiac conduction tissue was clearly distinguishable from the surrounding cardiac myocardium and connective tissue. Moreover, the histological information also navigated the anatomical architecture of the CCS and its location which providing an essential data for gross dissection.

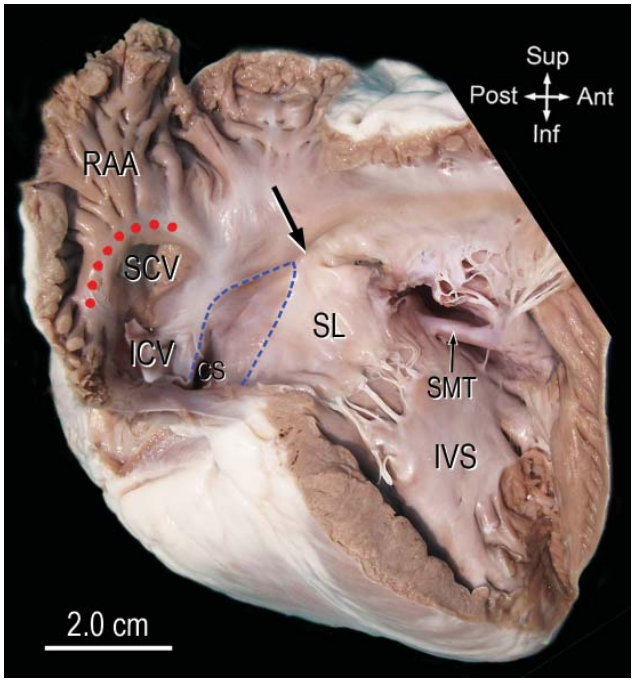

Figure 1. Photograph of endocardial aspect of the right atrium and right ventricle showing terminal crest (red dotted line) located between the right atrial appendage (RAA) and the superior and inferior venae cavae (SVC & IVC). The triangle of Koch is bounded by the attachment of the septal leaflet, the tendon of Todaro (blue dashed lines), and the coronary sinus (CS) orifice; IVS, interventricular septum; SMT, septomarginalis trabecula; arrow, membranous septum.

Sinoatrial Node (SAN)

With histological investigation, the SAN was embedded in epicardial connective tissue of the terminal sulcus (Figure 2). The individual nodal cells were smaller and slightly paler than the atrial working myocytes. Moreover, the node was enclosed by fibrous connective tissue and encircled around the sinoartrial node artery, allowing clearly distinguishable from the surrounding non-nodal tissue. From serial sections, the position of the SAN could be specified at lateral border of the terminal crest which adjoining to the sinus venarum. Furthermore, it extended from the superior cavoatrial junction to upper portion of the sinus venarum (Figure 3A, B & C).

At macroscopic level, the superior extremity of the SAN was recognized as a small epicardial ridge at the junction of the superior vena cava with the right atrial appendage. After removal of subepicardial tissue, the SAN was found to located at the junction between the musculature of the superior vena cava and the right atrial appendage (Figure 4A). The node was somewhat spindle in shape, and its inferior extremity extended toward the entrance of the inferior vena cava.

In 4 from 15 hearts, the identification of the SAN quite difficult so that the sinoatrial node artery was used as the clue to localize them. This was a principal arterial supply of the SAN. This artery was originated from the proximal part of the right coronary artery and then ran upward on the medial wall of the right atrium and directly toward the SAN (Figure 4B). The artery could be traced to the superior cavoatrial junction that led to the discovery of the SAN easily.

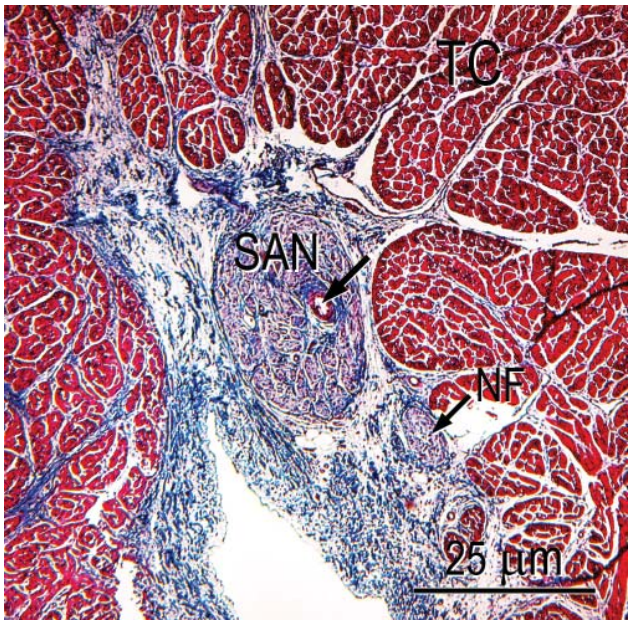

Figure 2. Micrograph of the section through the upper extremity of the sinoatrial node (SAN), corresponding to level A in Figure 3A. The node lying in subepicardial tissue of the terminal sulcus and enveloped with dense connective tissue. TC, terminal crest; arrow, branch of the sinoatrial node artery; NF, nerve fiber.

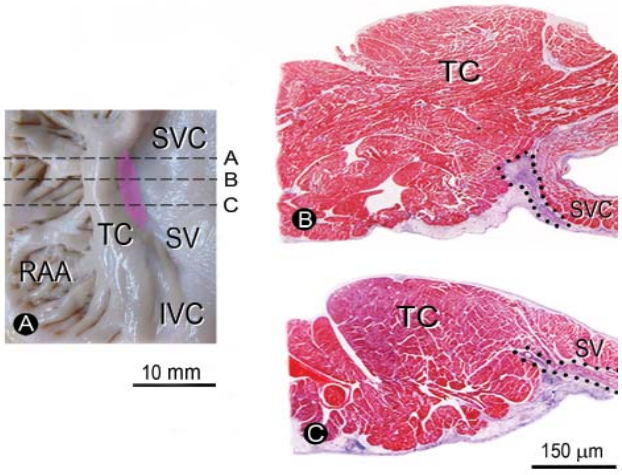

Figure 3. Photographs of the right atrial tissue block and sections of the sinoatrial node (SAN). A: Endocardial aspect of the cavoatrial junction showing the terminal crest (TC) situated between the sinus venarum (SV) and right atrial appendage (RAA), black dashed lines indicate levels of sections that made perpendicular to the long axis of the terminal crest and pass through the SAN (magenta area). B & C: The corresponding tissue sections at levels B and C showing the SAN lying subepicardial tissue within the terminal sulcus and its vicinity border marked with a black dotted line. IVC, inferior vena cava; SVC, superior vena cava.

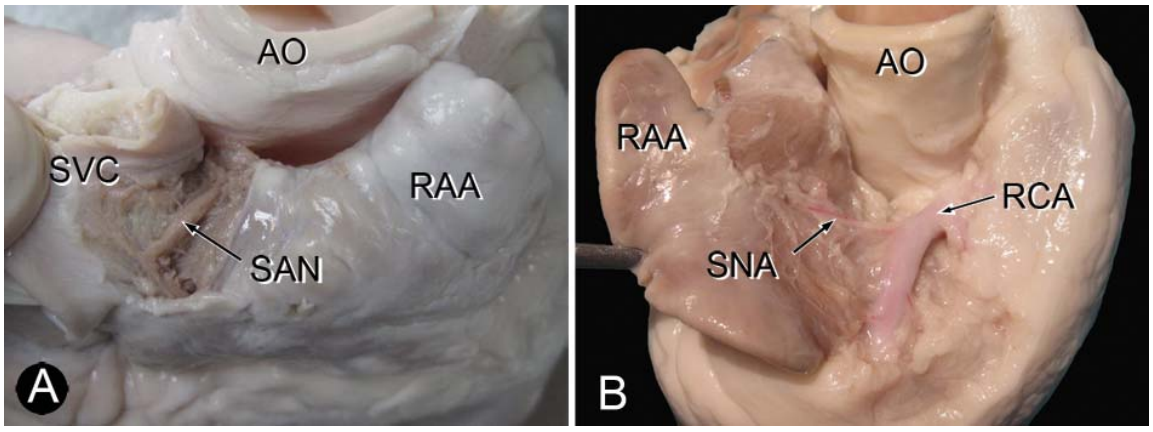

Figure 4. Photograph of the right supero-lateral aspect of the heart. A: The sinoatiral node (SAN) situated between the right atrial appendage (RAA) and superior vena cava (SVC). B: The sinoatrial node artery (SNA) branching from the right coronary artery (RCA) to supply the SAN. AO, aorta.

Atrioventricular (AV) Conduction Tissue

The atrioventricular (AV) conduction tissue consisted of the atrioventricular node (AVN), the atrioventricular (AV) bundle of His, the right and left bundle braches (RBB & LBB). The AV conduction tissue was sectioned perpendicular to the attachment of the septal leaflet of the tricuspid valve (Figure 5A). It was showed slightly paler staining than the working ventricular myocytes; therefore, it was clearly distinguishable from the surrounding ventricular muscle. The AVN was placed in subendocardial tissue of the atrioventricular junction, on the atrial surface of the central fibrous body (Figure 5B). Its upper border was blended with the cardiac myocytes of the interatrial septum, whereas the lower border merged with those of the interventricular septum. The distal extremity of the AVN extended into the central fibrous body so-called the penetrating bundle or the atrioventricular (AV) bundle of His (BH) (Figure 5C). This penetrating part was distinguished from the compact AVN at the point itself completely surrounded by the central fibrous body. A short segment of the BH was positioned on the summit of the muscular ventricular septum and encircled by thin collagenous connective tissue. At this region, the BH gave rise to the left bundle branch and the bundle itself continued as the right bundle branch (Figure 5D).

With gross dissection, the AV conduction tissue was easily distinguished from the surrounding cardiac myocytes and connective tissue on the basis of its whitish color (Figure 6A & B). After removal of the endocardial tissue at the apex of Koch's triangle, the AVN was identified (Figure 6A). It was an elliptical shaped and ensheathed by loose connective tissue. At the apex of the triangle of Koch corresponding to the membranous septum, the distal extremity of the AVN penetrated the central fibrous body to form the penetrating bundle of His (BH). Diameter of the BH was nearly constant in width and slightly smaller than the AVN. At the boundary between the membranous and muscular parts of the interventricular septum, the BH divided into the right and left bundle branches (RBB & LBB). The RBB continued down to the right ventricular aspect of the interventricular septum. Its initial segment was buried within the muscular part of the interventricular. Having reached the base of the anterior papillary muscle, it traveled along the septomarginal trabecula (Figure 6A).

The LBB passed through the lower rim of the membranous septum and arrived the endocardial surface of left ventricle at the commissure between the right coronary and non-coronary leaflets of the aortic valve (Figure 6B). Then it descended in the subendocardial tissue of the muscular part of interventricular septum, before distributed over the internal surface of the left ventricle as Purkinje fibers. The LBB could be directly observed under the ventricular endocardium as a whitish band compared with darker underling interventricular muscles.

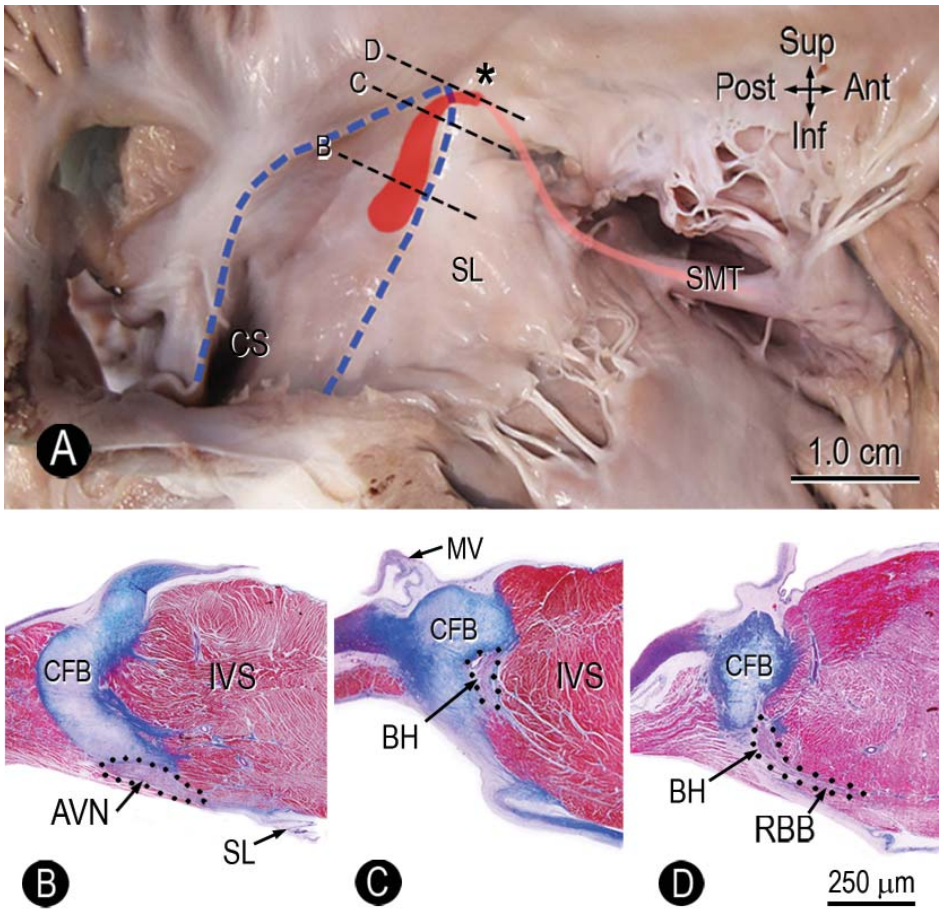

Figure 5. Photograph and micrographs of the atrioventricular junction. A: The atrioventricular node (orange area) locating at apex of triangle of Koch, black dashed lines indicate the levels of sectioned through the AV conduction tissue. The right bundle branch (light orange) coursing through the septomarginalis trabecula (SMT). B: The atrioventricular node (AVN) encountering at the atrioventricular junction. C:The penetrating bundle of His (BH) depositing in the connective tissue of the central fibrous body (CFB). D: The bundle of His (BH) branching into the right bundle branch (RBB). CS, coronary sinus; IVS, interventricular septum; MV, mitral valve; SL, septal leaflet of the tricuspid valve; *membranous septum.

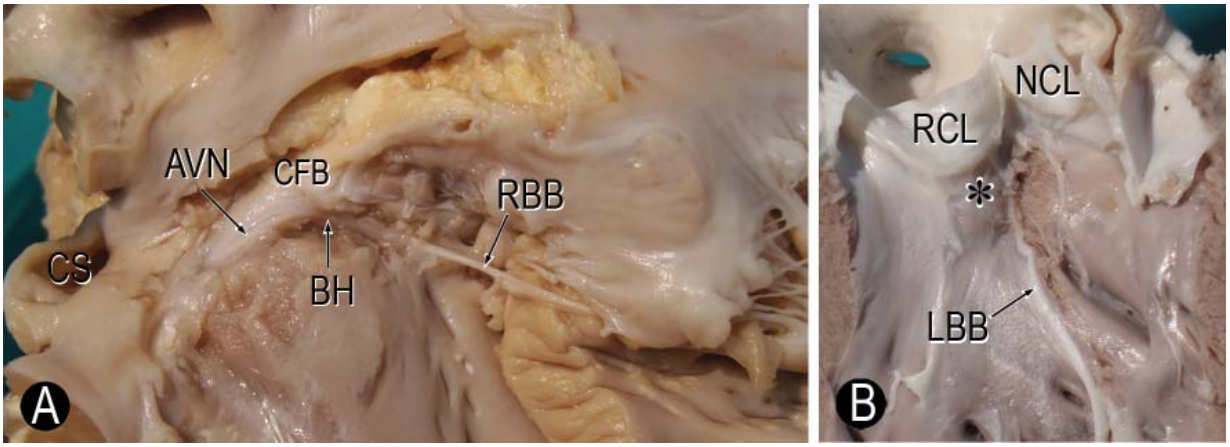

Figure 6. Photographs presenting the anatomical architectures of the cardiac conduction system. A: The bundle of His (BH) continuing from the atrioventricular node (AVN), passing through the central fibrous body (CFB) and bifurcating into the left and right bundle branches (RBB), which running through the septomarginalis trabecula. B: The left bundle branch (LBB) arriving the left ventricular chamber at the junction between the right coronary and non-coronary leaflets (RCL & NCL). CS, coronary sinus; *membranous septum.

DISCUSSION'

The present study shows that the anatomic architecture and specific location of the CCS in the pig heart are clearly demonstrated by gross anatomic dissection. Furthermore, the essential landmarks providing the ability to precisely dissect the CCS components were proposed.

Morphological variations of human SAN, resembling a triangle, horse-shoe, ellipse, or crescent depending on the forms of the sulcus terminalis, was proposed by Kawashima [14]. Moreover, the SAN in rabbit appeared as a thin layer of conducting cells [22]. By contrast the pig SAN revealed in the present study to be a spindle-shaped similar to that in human [9,10,18,19]. The differences of these findings may due to the ability of the investigation techniques. In addition, the cardiac specialized cells of the SAN was gradually blended with the surrounding atrial myocytes. Hence it is very difficult to specify the accurately border of the node in gross specimens. Although the morphology of the SAN varies among individuals, its position is almost constant. The superior cavoatrial junction has been a common location of the SAN in human [3,9,10,18,19], rabbit [22] and in pig. Therefore this area should be a crucial landmark for identification of the SAN. Moreover, another important structure is the sinoatrial node artery that could be used as a clue to locate the SAN during dissection [12,24].

It is generally accepted that the AVN situates at the apex of the triangle of Koch [1,3,5,6,14,23] which is confined by the attachment of the septal leaflet of the tricuspid valve anteriorly and the tendon of Todaro posteriorly [3]. The tendon of Todaro is inconveniently identified leading Kawashima and Sasaki [13] to propose the boundary between the membranous and muscular parts of the interventricular septum to be the crucial landmark for dissection of the AV conduction tissue. While in the present study, the septal leaflet was absolutely identified and it will navigate the location of the AVN. After the AVN obtained, the bundle of His and the RBB could be conveniently discovered. Thus, the worthy landmark for exploration of the AV conduction tissue should be the attachment of the septal leaflet adjoining the membranous septum. Moreover, the RBB is buried in the muscular tissue of the interventricular sepum and travels along the septomarginal trabecula similar to that of human [16].

The LBB in the pig is clearly observed as a whitish structure running in the subendocardium of the left ventricular surface of the interventricular septum as seen in human [13] and rabbit [4, 23]. As the LBB appears in the left ventricle at the junction between the right coronary and non-coronary leaflets of the aortic valve, this frontier should be a crucial landmark for its identification.

The regional anatomy of the CCS in relation to the surrounding structures is important not only for dissecting the CCS, but also as fundamental basis for improving the effective and safety of the catheter ablation of cardiac arrhythmias [8,19]. Moreover, the septal isthmus is the target to ablate the slow pathway in AV node reentrant tachycardia flutter and isthmus dependent atrial flutter [20]. This area is part of the right atrial vestibule located between the coronary sinus orifice and the attachment of the septal leaflet of the tricuspid valve.

CONCLUSION

The present study found that the crucial landmarks for the identification of the SAN, the AV conduction tissue and the LBB are the superior cavoatrial junction, the attachment of the septal leaflet adjoining the membranous septum, and the junction between the right coronary and non-coronary leaflets of the aortic valve, respectively. These landmarks are useful not only for gross anatomic dissection of the CCS in the pig heart, but also provide the fundamental information for cardiac arrhythmia and sudden death experimentation in this animal. It is obvious that these findings should be valuable for anatomists, cardiovascular researchers and veterinary clinicians, as well as veterinary and medical students.

SOURCES AND MANUFACTURERS

[1]Carl Ziess MicroImaging GmbH, Goettingen, Germany.

[2]Rushmore Precision Co., Ltd., Bangkok, Thailand.

***Funding*.** This work was financial supported by Khon Kaen University under the Incubation Researcher Project.

***Ethical approval*.** The study protocol has been reviewed and approved by the Animal Ethics Committee of Khon Kaen University, based on the Ethic of Animal Experimentation of National Research Council of Thailand (AEKKU 08/2553).

***Declaration of interest*.** The authors report no conflicts of interest. The authors alone are responsible for the content and writing of the paper.

REFERENCES

1 **Aanhaanen W.T., Mommersteeg M.T., Norden J., Wakker V., de Gier-de Vries C., Anderson R.H., Kispert A., Moorman A.F. & Christoffels V.M. 2010.** Developmental origin, growth, and three-dimensional architecture of the atrioventricular conduction axis of the mouse heart. *Circulation Research*. 107(6): 728-736.

2 **Akiyama T. 2010.** Sunao Tawara: Discoverer of the atrioventricular conduction system of the heart. *Cardiology Journal*. 17(4): 428-433.

3 **Anderson R.H., Boyett M.R., Dobrzynski H. & Moorman A.F.M. 2013.** The Anatomy of the Conduction System: Implications for the Clinical Cardiologist. *Journal of Cardiovascular Translational Research*. 6(2): 187-196.

4 **Atkinson A.J., Inada S., Li J., Tellez J.O., Yanni J., Sleiman R., Allah E.A., Anderson R.H., Zhang H., Boyett M.R. & Dobrzynski H. 2011.** Anatomical and molecular mapping of the left and right ventricular His–Purkinje conduction networks. *Journal of Molecular and Cellular Cardiology*. 51(5): 689-701.

5 **Atkinson A.J., Logantha S.J., Hao G., Yanni J., Fedorenko O., Sinha A., Gilbert S.H., Benson A.P., Buckley D.L., Anderson R.H., Boyett M.R. & Dobrzynski H. 2013.** Functional, anatomical, and molecular investigation of the cardiac conduction system and arrhythmogenic atrioventricular ring tissue in the rat heart. *Journal of the American Heart Association*. 2(6): 1-25.

6 **Bharati S., Levine M., Huang S.K., Handler B., Parr G.V., Bauernfetnd R. & Lev M. 1991.** The conduction system of the swine heart. *Chest*. 100(1): 207-212.

7 **Biondi-Zoccai G., De Falco E., Peruzzi M., Cavarretta E., Mancone M., Leoni O., Caristo M.E., Lotrionte M., Marullo A.G., Amodeo A., Pacini L., Calogero A., Petrozza V., Chimenti I., D'Ascenzo F. & Frati G. 2013.** A Novel Closed-Chest Porcine Model of Chronic Ischemic Heart Failure Suitable for Experimental Research in Cardiovascular Disease. *BioMed Research International*. 2013: 1-8.

8 **Cabrera J.A. & Sanchez-Quintana D. 2013.** Cardiac anatomy: what the electrophysiologist needs to know. *Heart*. 99(6): 417-31.

9 **Chander N., Aslanidi O., Buckley D., Inada S., Birchall S., Atkinson A., Kirk D., Monfred O., Molenaar P., Anderson R., Sharma V., Sigg D., Zhang H., Boyett M. & Dobrzynski H. 2011.** Computer three-dimentional anatomical reconstruction of the human sinus node and a novel paranodal area. *The Anatomical Record*. 294(6): 970-979.

10 **James T.N. 2002.** Structure and function of the sinus node, AV node and His bundle of the human heart: I-Structure. *Progress in Cardiovascular Diseases*. 45(3): 235-267.

11 **Kaese S., Frommeyer G., Verheule S., van Loon G., Gehrmann J., Breithardt G. & Eckardt L. 2013.** The ECG in cardiovascular-relevant animal models of electrophysiology. *Herzschrittmachertherapie and Elektrophysiologie*. 24(2): 84-91.

12 **Kawashima T. & Sasaki H. 2003.** The morphological significance of the human sinuatrial node branch (artery). *Heart and Vessels*. 18(4): 213-219.

13 **Kawashima T. & Sasaki H. 2005.** A macroscopic anatomical investigation of atrioventricular bundle locational variation relative to the membranous part of the ventricular septum in elderly human heart. *Surgical and Radiologic Anatomy*. 27(3): 206-213.

14 **Kawashima T. & Sasaki H. 2011.** Gross anatomy of the human cardiac conduction system with comparative morphological and developmental implications for human application. *Annals of Anatomy*. 193(1): 1-12.

15 **Keith A. & Flack M. 1907.** The form and nature of the muscular connections between the primary divisions of the vertebrate heart. *Journal of Anatomy and Physiology*. 41(Pt3): 172-189.

16 **Kosinski A., Grzybiak M., Nowinski J., Kedziora K., Kuta W., Dabrowska-Kugacka A., Lewicka E., Raczak G. & Kozłowski D. 2012.** Morphological remarks regarding the structure of conduction system in the right ventricle. *Kardiologia Polska*. 70(5): 472-476.

17 **Koudstaal S., Jansen of Lorkeers S., Gho JM., van Hout G.P., Jansen M.S., Gründeman P.F., Pasterkamp G., Doevendans P.A., Hoefer I.E. & Chamuleau S.A. 2014.** Myocardial infarction and functional outcome assessment in pigs. *Journal of Visualized Experiments*. (86): 1-10.

18 **Sanchez-Quintana D., Cabrera J.A., Farre J., Climent V., Anderson R.H. & Ho S.Y. 2005.** Sinus node revisited in the era of electroanatomical mapping and catheter ablation. *Heart*. 91(2): 189-194.

19 **Sanchez-Quintana D., Pizarro G., Lopez-Minguez J.R., Ho S.Y. & Cabrera J.A. 2013.** Standardized Review of Atrial Anatomy for Cardiac Electrophysiologists. *Journal of Cardiovascular Translational Research*. 6(2): 124-144.

20 Saremi F., Torrone M. & Yashar N. 2009. Cardiac conduction system: delineation of anatomic landmarks with multi-detector CT. *Indian Pacing and Electrophysiology Journal*. 9(6): 318-333.

21 Silverman M.E., Grove D. & Upshaw Jr. C.B. 2006. Why does heart beat? The discovery of the electrical system of the heart. *Circulation*. 113(23): 2775-2781.

22 Stephenson R.S., Boyett M.R., Hart G., Nikolaidou T., Cai X., Corno A.F., Alphonso N., Jeffery N. & Jarvis J.C. 2012. Contrast Enhanced Micro-Computed Tomography Resolves the 3-Dimensional Morphology of the Cardiac Conduction System in Mammalian Hearts. *PLos ONE*. 7(4): 1-11.

23 Suzuki Y., Yeung A.C. & Ikeno F. 2011. The Representative Porcine Model for Human Cardiovascular Disease. *Journal of Biomedicine and Biotechnology*. 2011: 1-10.

24 Yanagawa N. & Nakjima Y. 2009. A simple dissection method for the conduction system of the human heart. *Anatomical Sciences Education*. 2(2): 78-80.